ERDC/TN DOER-N17
August 2022

Development of a Three-Dimensional Vegetative Loss Mechanism for the Geophysical Scale Transport Multi-Block Hydrodynamic Sediment and Water Quality Transport Modeling System (GSMB)

by Ray Chapman[1], Phu Luong[2], Sung-Chan Kim[2], and Earl Hayter[3]

PURPOSE: The US Army Engineer Research and Development Center's (ERDC) Environmental Laboratory (EL) and Coastal and Hydraulics Laboratory (CHL) have completed several large scale hydrodynamic, sediment and water quality transport studies. These studies have been successfully executed utilizing the Geophysical Scale Transport Modeling System (GSMB), which is composed of multiple process models (Figure 1). Due to being directly and indirectly linked within the GSMB framework, the US Army Corps of Engineers (USACE) accepted wave, hydrodynamic, sediment, and water quality transport models are both directly and indirectly linked within the GSMB framework.

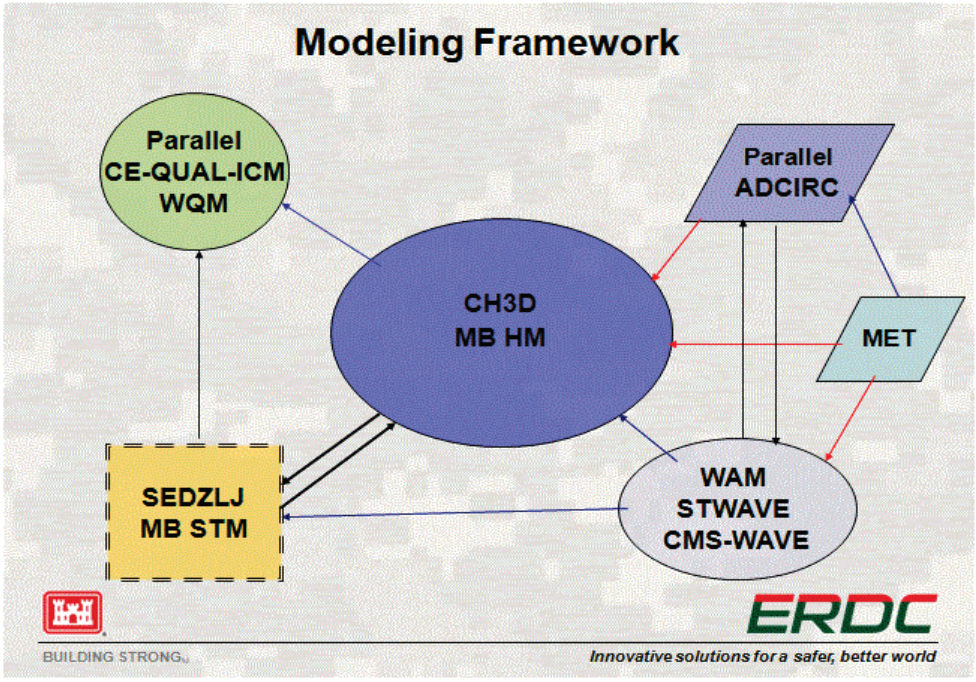

Figure 1. Multi-block geophysical scale transport modeling system.

[1] Ray Chapman & Associates, raychapmanandassoc@gmail.com.
[2] Coastal and Hydraulics Laboratory, US Army Engineer Research and Development Center.
[3] Environmental Laboratory, US Army Engineer Research and Development Center.

BACKGROUND: Components of the GSMB are listed below.

1. Two-dimensional (2D) deep water wave model WAM (The Wave Model) (Komen et al. 1994; Jensen et al. 2012)

2. Data from meteorological model (e.g., Saha et al. 2010 - http://journals.ametsoc.org/doi/pdf/10.1175/2010BAMS3001.1)

3. Shallow water wave models STWAVE (Smith et al. 1999; Massey et al. 2011)

4. CMS-WAVE (Lin et al. 2008)

5. Large scale unstructured 2D ADCIRC hydrodynamic model (http://www.adcirc.org)

6. Regional scale models CH3D-MB (Luong and Chapman 2009); the multi-block (MB) version of CH3D-WES (Chapman et al. 1996; Chapman et al. 2009), MB CH3D-SEDZLJ sediment transport model (Hayter et al. 2012), and CE-QUAL Management-ICM water quality model (Bunch et al. 2003; Cerco and Cole 1994)

Task 2 of the Dredging Operations and Environmental Research (DOER) project "Modeling Transport in Wetting/Drying and Vegetated Regions" is to implement and test a three-dimensional (3D) vegetative loss mechanism within GSMB. This technical note (TN) describes the methods implemented representing vegetative effects and results from test cases.

VEGETATIVE LOSS MECHANISM IMPLEMENTATION: A common approach to represent vegetative losses in the equations of motion is including a bulk frictional and form drag a loss term.

$$F_{vi} = \tfrac{1}{2}\lambda C_d U_i \left|U\right|$$

where U_i is the horizontal velocity vector, C_d is the drag coefficient, and λ is vegetative density. The vegetative density is the fraction of a volume of a computation cell occupied by vegetation. This can also be expressed as $\lambda = nD$, where n is the number of stems per computational cell and D is the individual stem diameter. A thorough review of the vegetative loss mechanism and related work is presented in Nepf (1999), Nepf and Vivoni (2000), and Nepf (2012).

In the input files MAIN.INP and vegfac-blk#.inp within the GSMB an aggregate vegetative loss coefficient $C_{v,} = \tfrac{1}{2}\lambda C_d$ can be defined on a computational cell-by-cell basis and block-by-block basis. Within MAIN.INP, RSPAC(5) is the individual stem diameter in centimeters, D, RSPAC(6) is the number of stems per cell, n, scaled by 1,000,000 and the drag coefficient; C_d is specified in the input file vegfac-blk#.inp. This approach allows for spatially varying vegetative density and drag coefficients within the GSMB.

Within the GSMB, the vegetative loss forces are applied explicitly in subroutines CH2DXADIW and CH2DYADIW when the water column depth exceeds HMINW (RSPAC(7) in MAIN.INP). Similarly, the loss forces are applied explicitly in CH3DXYZWDV when the water column depth exceeds HMINWD (RSPAC(8) in MAIN.INP).

Here, it is assumed the reader is familiar with the mechanics of two-equation turbulence modeling and specifically, the implementation of vertical k – ε transport as presented in Chapman et al. (1996). The effect of vegetation on turbulent transport has been implemented in the k – ε turbulence model subroutine of the CH3D MB-HM model, CH3DKEV, where additional turbulence production and dissipation parameterizations are introduced similar to that investigated by Lopez and Garcia (1997, 1998, and 2001).

Scalar production of turbulence due to vegetative resistance is defined as:

$$P_{vtk} = C_v |U|^3$$

Similarly, the scalar dissipation of turbulence due to vegetative resistance is defined as:

$$P_{vt\varepsilon} = 1.44\ (\varepsilon / k)\ C_v |U|^3$$

Works such as Katul (2004), Jahra et al. (2011), and Soulitios and Panyios (2001) recognized the effect of wake turbulence interference and modified the vegetative production and dissipation so that

$$P_{vtk} = C_v |U|^3 - C_k |U| k$$

and

$$P_{vt\varepsilon} = 1.44\ (\varepsilon / k)\ C_v |U|^3 - C_\varepsilon |U| \varepsilon$$

where C_k is the fraction of mean flow kinetic energy converted to turbulence energy, k, by wake formation; C_ε controls the fraction of k dissipated. In general, they represent adjustable parameters set to control unbounded growth of turbulence energy, where $0.0 < C_k < 1.0$ and $1.0 < C_\varepsilon < 5.0$.

These modifications to the k-ε turbulent transport subroutine alter the computed longitudinal and vertical distribution of the turbulent eddy viscosity for momentum transport and eddy diffusivity for salt, temperature, and sediment transport.

VEGETATIVE LOSS MECHANISM TESTING: A series of test simulations were designed to evaluate the vegetative loss mechanism on both mean flow and turbulent transport. Initial testing of this algorithm was performed by simulating flow in a single computational block flume that was two cells wide, 60 cells in length, and had a nine-layer sigma stretched vertical grid. Grid size was 200 m wide by 200 m long, resulting in flume dimensions of 400 m wide and 12,000 m long and a constant depth of 1.5 m (Figure 2).

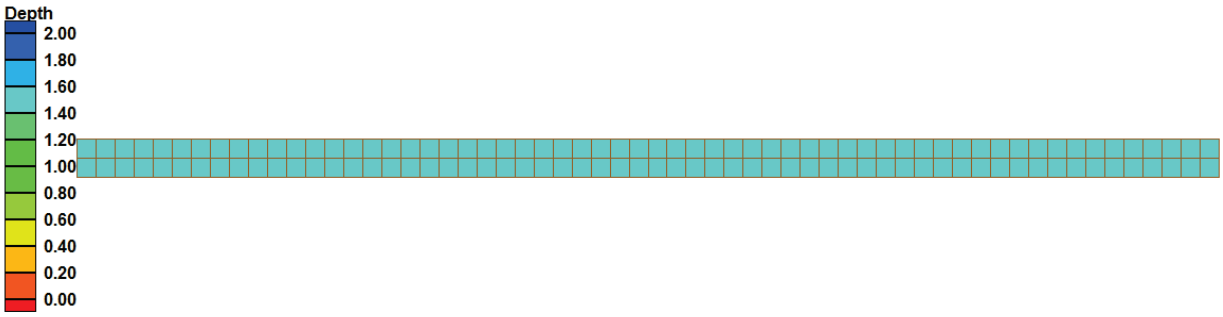

Figure 2. East oriented grid and bathymetry.

A 2-m range, 24-hour sinusoidal tide boundary is specified at the west end of the flume. As stated above, the effect of vegetation on the simulation within the GSMB is introduced through specification D, the individual stem diameter (RSPAC(5)), n, the number of stems per computational cell (RSPAC(6)) and the vegetative form drag coefficient, C_d, which is defined on a computational cell-by-cell basis in vegfac-blk01.inp (a control file for CH3D-MB). The fraction of vegetative coverage is the area of stems scaled by the area of a computational cell. In this case, D = 1.128 cm, which corresponds to an approximate stem area of 1 cm^2 and n varies from 0 to 200, in which a value of n = 200 represents 50% vegetative cover. Spatially varying form drag specified in vegfac-blk01.inp was set to 0.0 in the first 40 cells or no vegetation through 8,100 m and 0.8 in the remaining cells. The selection of the above parameter is reasonable and within the limits of available measurements, however, purely arbitrary.

Figure 3 shows the effect of vegetative density on the temporal water surface response. It presents a comparison of the water surface elevation response at cell 55, or X = 10900 for 0, 5, and 25% vegetative coverage. This clearly shows an increasing phase shift and amplitude loss due to enhance form drag.

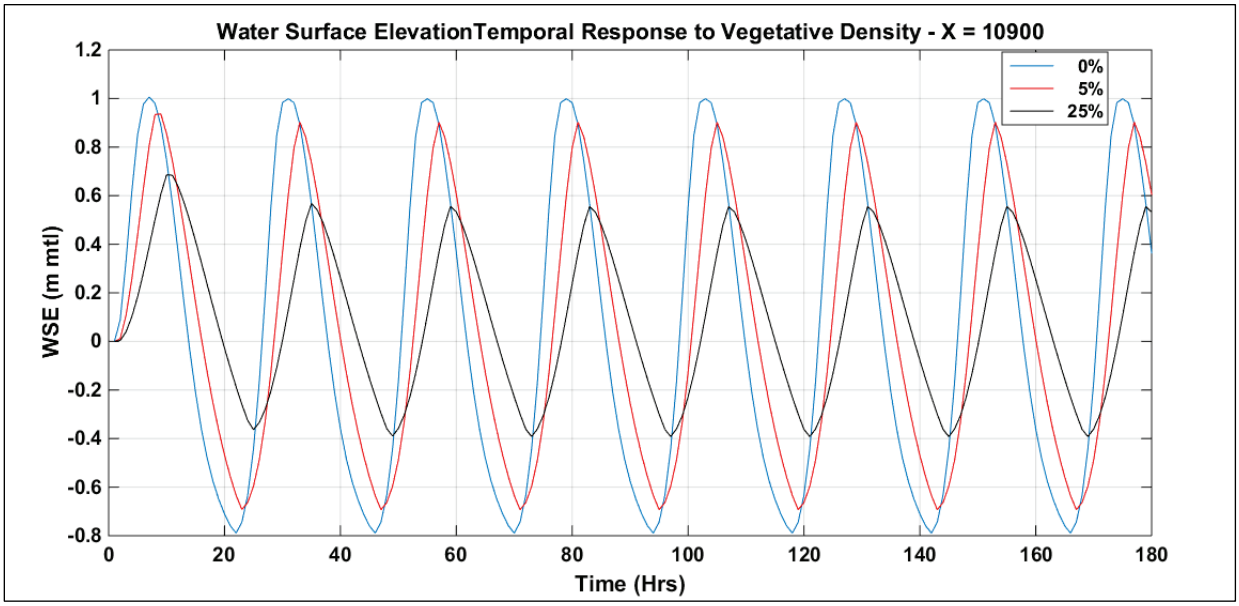

Figure 3. WSE response at cell 55, X = 6,900 m for varying coverage.

Figures 4 and 5 show the effect of vegetative density on velocity profile. A comparison of the maximum velocity profiles at cell 35, or X = 6,900 m for 0.0%, 5%, and 25% vegetative density is presented in Figure 4. For both flood and ebb tide, the vertical velocity distribution of velocity exhibits a decrease in magnitude and gradient with increasing vegetative density. A similar, but most pronounced response is seen in Figure 5, where the maximum velocity profiles at cell 55, or X = 10,900 m is presented. Not only are the magnitudes reduced, but the vertical profiles are also homogenized by increased turbulent mixing generated by the form drag contribution to the k-ε transport model.

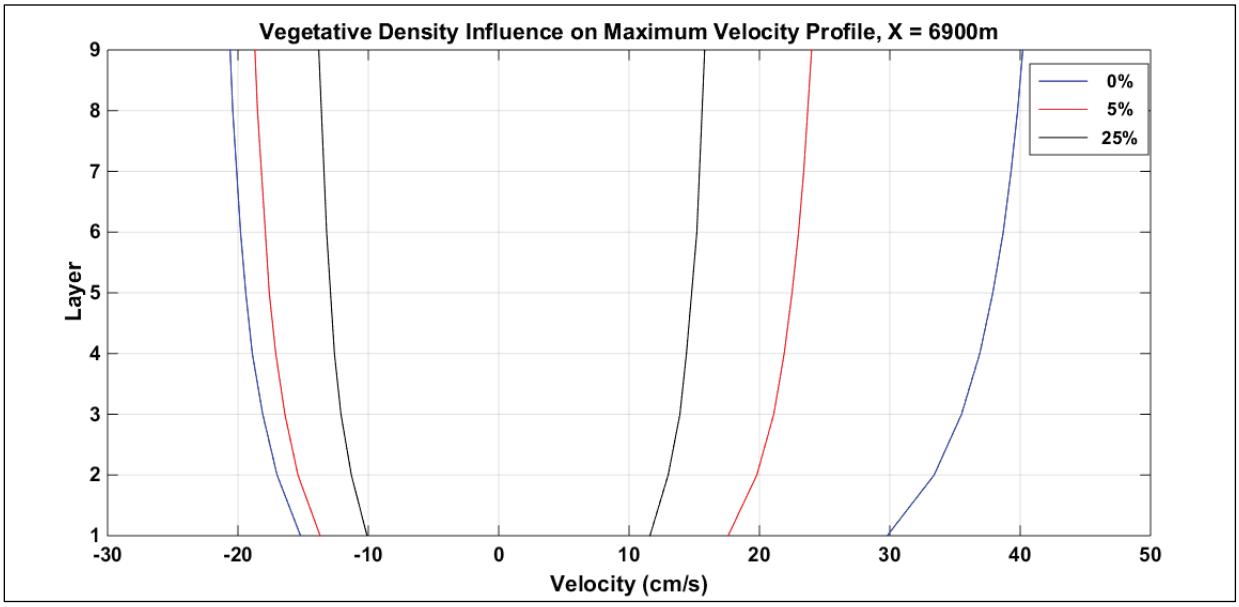

Figure 4. Vertical velocity profile response at Cell 35, X = 6,900 m.

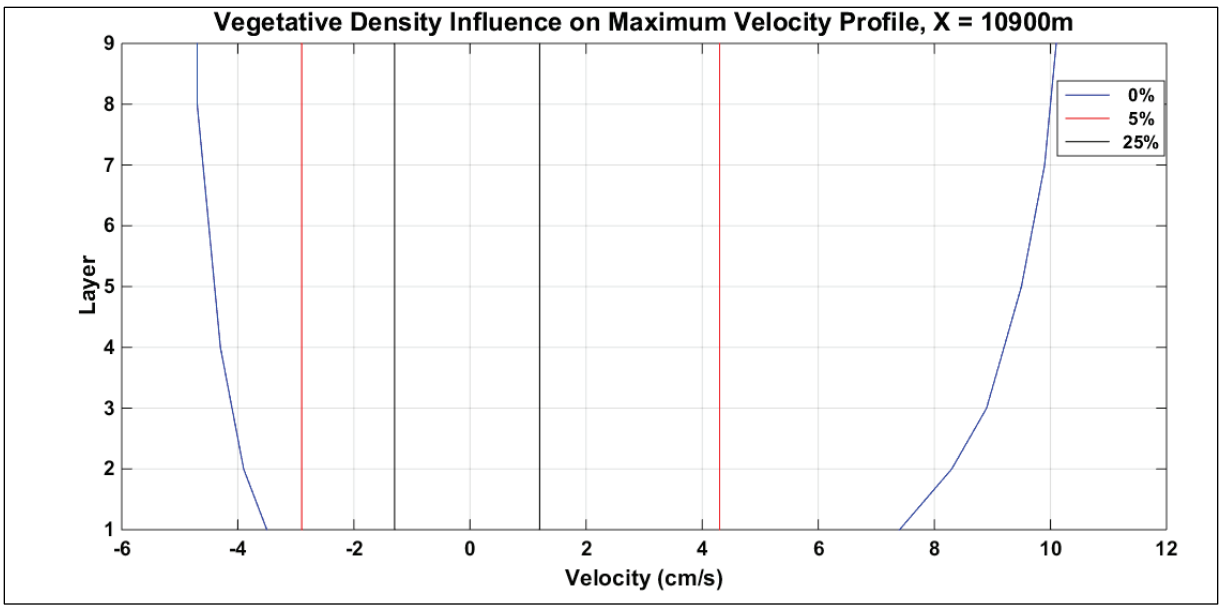

Figure 5. Vertical velocity profile response at Cell 55, X = 10,900 m.

This behavior can be explained by examining the predicted turbulent eddy viscosity distributions and the influence of vegetative density. The vertical profiles of maximum turbulent eddy viscosity for 0, 25, and 25% vegetative coverage in the channel reach without vegetation at X = 6,900 m can be seen in Figure 6. The expected parabolic form generated by the k-ε transport model decreases in magnitude with the presence of downstream vegetative coverage due to the decrease in velocity magnitude and gradient shown in Figure 5.

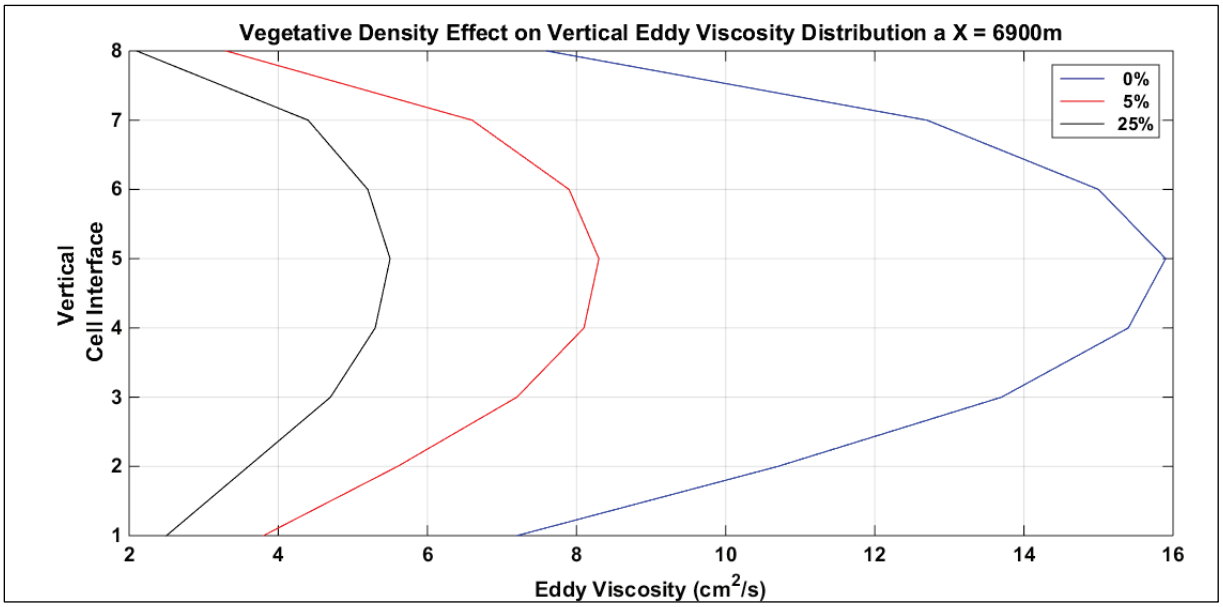

Figure 6. Maximum Vertical eddy viscosity distribution at Cell 35, X = 6,900 m.

Figure 7 shows profiles of maximum turbulent eddy viscosity for 0, 1, 5, and 25% vegetative coverage in the channel reach with vegetation at X = 10,900 m. Much like the homogenized vertical velocity profiles (Figure 5), the eddy viscosity distributions become more vertically uniform with increased form drag and wake production. There is a noticeable but small increase in the magnitude of maximum eddy viscosity when the vegetative density is increased from 1 to 5%, however, an increase to 25% indicates that wake production and dissipation overwhelms the turbulent production due to form drag. It must be kept in mind that the k – ε code modifications are based on empirical formulations and data analysis, so trends in modification of the mixing regime should be considered as opposed to absolute numbers.

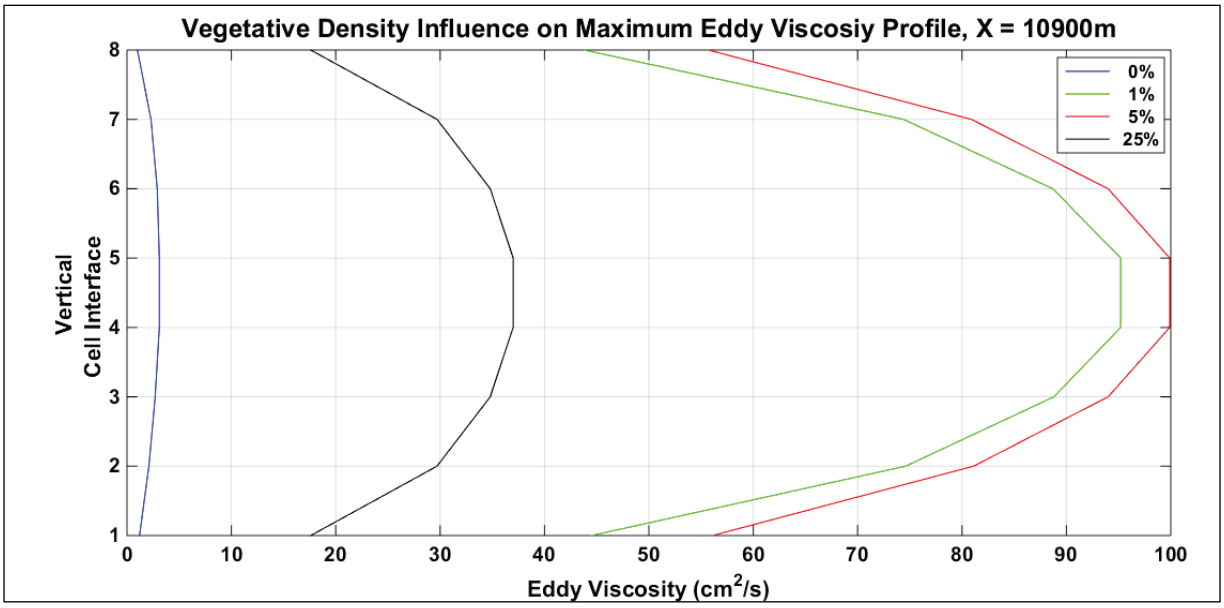

Figure 7. Maximum vertical eddy viscosity distribution at Cell 55, X = 10,900 m.

Further insight can be gained by examining the temporal variation of the mid-depth turbulent eddy viscosity (Figure 8) for 5, 25, and 50.0% vegetative coverage. As also observed in Figure 7, the maximum value of the mid-depth turbulent eddy viscosity is highly dependent on vegetative density as well as phase of the tide. Specifically, as the vegetative density increases the velocity decreases resulting in less shear, form drag, and mixing.

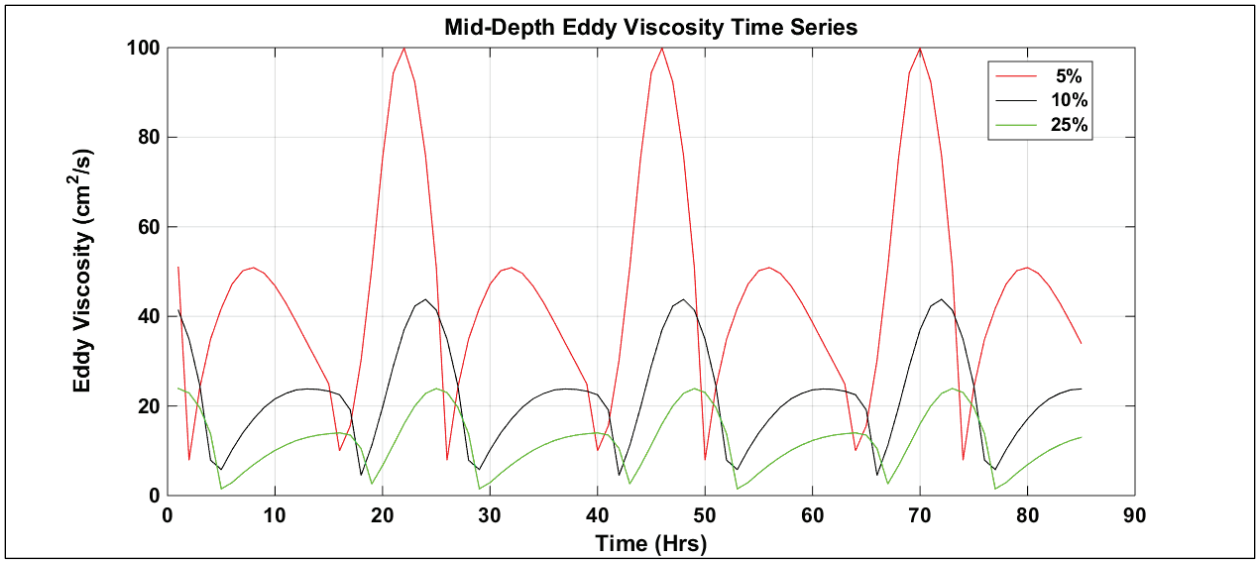

Figure 8. Temporal variation of mid-depth viscosity distribution at Cell 55, X = 10,900 m.

SUMMARY: A 3D vegetative loss mechanism has been successfully implemented within the hydrodynamic and turbulent transport modules of GSMB. It has been shown that the modeled water surface elevation, velocity, and turbulent eddy viscosity are significantly influenced by

vegetative density. As a result, the mixing and transport of salt, temperature, and sediment will be dependent on the proper characterization of this mechanism.

REFERENCES

Bunch, B. W., M. Channel, W. D. Corson, B. A. Ebersole, L. Lin, D. J. Mark, J. P. McKinney, S. A. Pranger, P. R. Schroeder, S. J. Smith, D. H. Tillman, B. A. Tracy, M. W. Tubman, and T. L. Welp. 2003. *Evaluation of island and nearshore confined disposal facility alternatives, Pascagoula River Harbor Dredged Material Management Plan*. ERDC-03-3. Vicksburg, MS: US Army Engineer Research and Development Center.

Cerco, C., and T. Cole. 1994. *Three-dimensional eutrophication model of Chesapeake Bay*. ERDC/EL TR-94-4. Vicksburg, MS: US Army Engineer Waterways Experiment Station.

Chapman, R. S., B. H. Johnson, and S. R. Vemulakonda. 1996. Users guide for the sigma stretched version of CH3D-WES; A three-dimensional numerical hydrodynamic, salinity and temperature model. Technical Report HL-96-21. Vicksburg, MS: U.S. Army Engineer Waterways Experiment Station.

Hayter E. J., R. S. Chapman, P. V. Luong, S. J. Smith, and D. B. Bryant. 2012. *Demonstration of predictive capabilities for fine-scale sedimentation patterns within the port of Anchorage, AK*. Final Report prepared for US Army District, Anchorage, AK.

Jahra, F., T. Kawahara, and F. Hasegawa. 2011 "Performance of a turbulence model for flows in partially vegetated open channels." *Journal of Japan Society of Civil Engineers, Series B1, Hydraulic Engineering* 67(4): I_193-I_198.

Jensen, R. E., M. A. Cialone, R. S. Chapman, B. E. Ebersole, M. Anderson, and L. Thomas. 2012. *Modeling of Lake Michigan storm waves and water levels*. ERDC/CHL TR-12-26. Vicksburg, MS: US Army Engineer Research and Development Center.

Katul, G. G., L. Mahrt, D. Poggi, and C. Sanz. 2004. "One- and two-equation models for canopy turbulence." *Boundary-Layer Meteorology* 113: 81-109.

Komen, G. J., L. Cavaleri, M. Donelan, K. Hasselmann, S. Hasselmann, and P. A. E. M. Janssen. 1994. *Dynamics and Modelling of Ocean Waves*. Cambridge University Press, Cambridge.

Lin, L., Z. Demirbilek, H. Mase, J. Zheng, and F. Yamada. 2008. *CMS-Wave: A nearshore spectral wave processes model for coastal inlets and navigation projects*. ERDC/CHL TR-08-13. Vicksburg, MS: US Army Engineer Research and Development Center.

Lopez, F., and M. Garcia. 1997. *Open-Channel Flow through Simulated Vegetation: Turbulence Modeling and Sediment Transport, Wetlands Research Program Rep*. WRP-CP-10. Washington, DC: US Army Corps of Engineers.

Lopez, F., and M. Garcia. 1998. "Open-channel flow through simulated vegetation: Suspended sediment transport modeling." *Water Res. Res.* 34(9): 2341–2352.

Lopez, F., and M. H. Garcia. 2001. "Mean flow and turbulence structure of open-channel flow through non-emergent vegetation." *J. Hydraul. Eng*. 127(5)**:** 392-402.

Luong, P. V., and R. S. Chapman. 2009. *Application of Multi-Block Grid and Parallelization Techniques in Hydrodynamic Modeling DoD High Performance Computing Modernization Program: User Group Conference* (HPCMP-UGC), San Diego, CA.

Massey, T. C., M. E. Anderson, J. M. Smith, J. Gomez, and R. Jones. 2011. *STWAVE: Steady –State Spectral Wave Model User's Manual for STWAVE, Version 6.0*. ERDC/CHL-SR-11-1. Vicksburg, MS: US Army Engineer Research and Development Center.

Nepf, H. M. 1999. "Drag, turbulence, and diffusion in flow through emergent vegetation." *Water Resources Research* 35 (2): 479–489.

Nepf, H. M., and E. R. Vivoni. 2000. "Flow structure in depth-limited, vegetated flow." *Journal of Geophysical Research* 105(28):547-28,557.

Nepf, H. M. 2012. "Flow and transport in regions with aquatic vegetation." *Annual Review of Fluid Mechanics* 44: 123-142.

Smith, J. M., D. T. Resio, and A. K. Zundel. 1999. *STWAVE: Steady-State Spectral Wave Model; Report 1: User's manual for STWAVE version 2.0*. ERDC/CHL SR-99-1. Vicksburg, MS: US Army Engineer Research and Development Center.

Souliotis, D., and P. Panayotis. 2011. "Effect of a Vegetation Patch on Turbulent Channel Flow." *Journal of Hydraulic Research* 49:2, 157-167.